Complex DDI by Fenebrutinib and the Use of Transporter Endogenous Biomarkers to Elucidate the Mechanism of DDI

Nicholas S. Jones[1,†], Kenta Yoshida[2,†], Laurent Salphati[3], Jane R. Kenny[3], Matthew R. Durk[3] and Leslie W. Chinn[2,*]

Mechanistic understanding of complex clinical drug–drug interactions (DDIs) with potential involvement of multiple elimination pathways has been challenging, especially given the general lack of specific probe substrates for transporters. Here, we conducted a clinical DDI study to evaluate the interaction potential of fenebrutinib using midazolam (MDZ; CYP3A), simvastatin (CYP3A and OATP1B), and rosuvastatin (BCRP and OATP1B) as probe substrates. Fenebrutinib (200 mg) increased the area under the curve (AUC) of these probe substrates twofold to threefold. To evaluate the mechanism of the observed DDIs, we measured the concentration of coproporphyrin I (CP-I) and coproporphyrin III (CP-III), endogenous biomarkers of OATP1B. There was no change in CP-I or CP-III levels with fenebrutinib, suggesting that the observed DDIs were caused by inhibition of CYP3A and BCRP rather than OATP1B, likely due to increased bioavailability. This is the first published account using an endogenous transporter biomarker to understand the mechanism of complex DDIs involving multiple elimination pathways.

Study Highlights

WHAT IS THE CURRENT KNOWLEDGE ON THE TOPIC?

☑ Endogenous biomarkers are becoming important tools to evaluate transporter function alteration in humans, thus providing early liability assessment for transporter-mediated drug–drug interactions (DDIs) for investigational drugs.

WHAT QUESTION DOES THIS STUDY ADDRESS?

☑ Can we use endogenous biomarkers to understand the mechanism of complex DDIs that involve multiple elimination processes using clinical DDI with fenebrutinib as an example?

WHAT DOES THIS STUDY ADD TO OUR KNOWLEDGE?

☑ The study suggested that fenebrutinib is a clinical inhibitor of CYP3A and BCRP, but not OATP1B, based on the totality of evidence from clinical DDIs with probe substrates and endogenous biomarkers.

HOW MIGHT THIS CHANGE CLINICAL PHARMACOLOGY OR TRANSLATIONAL SCIENCE?

☑ This study demonstrates a new approach of utilizing endogenous biomarkers to evaluate complex DDIs and can lead to better strategy for DDI management based on mechanistic understanding.

The importance of understanding transporter-mediated drug–drug interactions (DDIs) is highlighted by the fact that transporters play a critical role in the absorption, distribution, metabolism, and excretion of drugs.[1] Regulatory agencies recognize the role of transporters in the context of new drug development, and their guidelines recommend the evaluation of transporter-mediated DDIs.[2–4] There are certain challenges, however, in the risk assessment of transporter-mediated DDIs. Typically, the initial assessment of DDI potential for a new molecular entity as perpetrator utilizes *in vitro* experiments and applies "basic" models in which *in vitro* parameters (such as inhibition constants (K_i) or half-maximal inhibitory concentration (IC_{50})) are compared with the clinical exposure of an new molecular entity. It has been reported that these basic models can cause false-positive predictions, leading to unnecessary clinical studies to evaluate DDI potential.[5] Another challenge is the general lack of specific substrates or inhibitors for transporters,[1] which can make the interpretation of observed clinical DDIs challenging when multiple transporters can be involved in the interaction.

To address these issues, there is currently major interest in the utilization of endogenous compounds as biomarkers for transporter

[1]Clinical Science, Genentech, Inc., South San Francisco, California, USA; [2]Clinical Pharmacology, Genentech, Inc., South San Francisco, California, USA; [3]Drug Metabolism and Pharmacokinetics, Genentech, Inc., South San Francisco, California, USA. *Correspondence: Leslie Chinn (chinn.leslie@gene.com)

[†]These authors contributed equally to this work.

Received June 5, 2019; accepted July 29, 2019. doi:10.1002/cpt.1599

function to better predict transporter-mediated DDIs.[6] One potential biomarker is coproporphyrin I (CP-I), with clinical data that support its utility in OATP1B DDI risk assessment. CP-I and CP-III are metabolites of heme that are produced at a relatively constant rate in healthy individuals. CP-I and CP-III are taken up by OATP1B1 and OATP1B3 at the basolateral membrane of hepatocytes and subsequently may be excreted into bile via MRP2 or undergoe basolateral efflux via MRP3. It was previously demonstrated that CP-I and CP-III are specific substrates for OATP1B1 and OATP1B3, with OATP2B1 also contributing to CP-III uptake.[7] CP plasma concentrations increase in conditions of reduced OATP activity, as seen in Rotor syndrome or through coadministration with OATP1B inhibitors.[6]

Fenebrutinib (GDC-0853) is a highly selective, orally administered, reversible inhibitor of Bruton's tyrosine kinase, a key kinase in signaling cascades following B-cell-antigen receptor activation in B cells that has recently become a focus of development as a potential target for immunosuppression in the treatment of autoimmune disorders and for B-cell neoplasms.[8] Fenebrutinib has been evaluated in phase I studies, including single-ascending and multiple-ascending dose studies, and it showed target engagement at plasma concentrations of 100 nM and a terminal half-life ($t_{1/2}$) of 4–10 hours.[9] Fenebrutinib is currently being evaluated in phase II studies in patients with rheumatoid arthritis, systemic lupus erythematous, and chronic spontaneous urticaria.

Patients with chronic autoimmune conditions often have comorbidities from chronic inflammation (e.g., high risk of cardiovascular disease in patients with lupus). The high prevalence of use of concomitant medications, such as statins, requires understanding of the DDI potential of fenebrutinib via metabolic enzymes and transporters. For example, the pharmacokinetics (PKs) of rosuvastatin are determined by multiple transporters, including OATP1B, OATP2B1, NTCP, BCRP, and MRP4.[10–12] OATP1B is important for hepatic uptake of rosuvastatin (with NTCP and OATP2B1 thought to play a lesser role), and inhibition of this transporter could increase the risk of exposure-dependent toxicities.[13] In contrast, BCRP is an efflux transporter, and inhibition of this transporter could increase both hepatic and plasma rosuvastatin concentrations, resulting in the potential for increased hepatic exposure as well as toxicity.

Here, we conducted *in vitro* and clinical studies to evaluate enzyme-mediated and transporter-mediated DDI of fenebrutinib as an inhibitor. In the clinical study, midazolam (MDZ; CYP3A), simvastatin (CYP3A and OATP1B), and rosuvastatin (BCRP and OATP1B) were used as probe substrates. To further evaluate the mechanism of observed clinical DDI, we measured CP-I, an endogenous biomarker of OATP1B activity. Our results demonstrate that CP-I can serve as a biomarker for DDIs in interactions involving OATP1B and can aid in the determination of the underlying mechanism of a DDI.

RESULTS

In vitro transporter inhibition

OATP1B1, OATP1B3, and OAT3. Fenebrutinib inhibited the OATP1B1-mediated and OATP1B3-mediated accumulation of the probe substrates ß-estradiol 17-(ß-D-glucuronide) ($E_2$17ßG) and cholecyctokinine-8 (CCK-8), respectively, in a concentration-dependent manner, with maximum inhibition observed at 30 µM of 62.8% and 86.7%, respectively (**Figure 1**). The calculated IC_{50} values were 19.7 µM for OATP1B1 and 7.15 µM for OATP1B3. Fenebrutinib did not influence the OAT3-mediated accumulation of the probe substrate estrone-3-sulfate up to 30 µM, the highest concentration tested (data not shown).

BCRP

Fenebrutinib inhibited the BCRP-mediated efflux ratio of prazosin across MDCKII-BCRP monolayers in a concentration-dependent manner (**Figure 1**). The IC_{50} of fenebrutinib for prazosin transport was calculated to be 9.40 µM.

In vitro CYP inhibition in human liver microsomes

No reversible or time-dependent inhibition (TDI) was observed on CYP1A2, CYP2B6, CYP2C8, CYP2C9, CYP2C19, and CYP2D6 at concentrations up to 15 µM (CYP2C19 and CYP2D) or 50 µM (all other isoforms tested). Additionally, no reversible CYP3A inhibition was observed using both MDZ and testosterone (TST) as probe substrates, but TDI was observed. The TDI kinetic parameters of fenebrutinib at CYP3A were as follows: using MDZ as a probe k_{inact} and apparent K_i were 0.0114 min^{-1} and 7.9 µM, respectively. Using TST as a probe, the k_{inact} and apparent K_i were 0.015 min^{-1} and 10.8 µM, respectively.

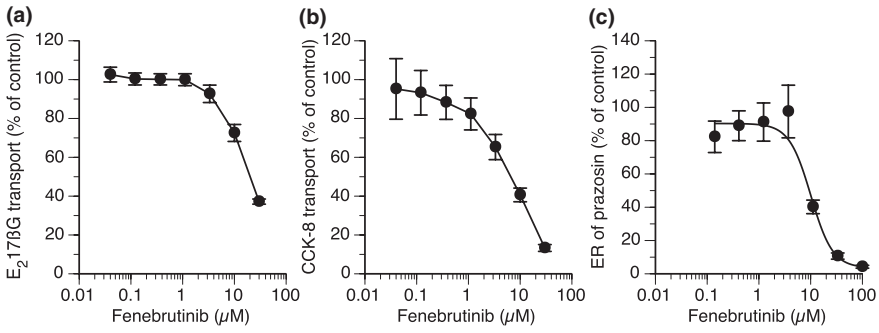

Figure 1 *In vitro* inhibition of transporter function by fenebrutinib. (**a**) Inhibition of ß-estradiol 17-(ß-D-glucuronide) ($E_2$17ßG) transport by fenebrutinib in HEK293 cells expressing OATP1B1. (**b**) Inhibition of cholecyctokinine-8 (CCK)-8 transport by fenebrutinib in HEK293 cells expressing OATP1B3. (**c**) Inhibition of prazosin ER by fenebrutinib in MDCKII cells expressing BCRP. Circles and vertical bars represent arithmetic means and SDs (n = 3). ER, efflux ratio.

Effect of multiple doses of fenebrutinib on the PKs of MDZ and 1'-hydroxymidazolam

The effect of multiple doses of fenebrutinib (200 mg b.i.d.) on the plasma concentration-time profiles of the CYP3A substrate MDZ and its metabolite 1'-hydroxymidazolam are presented in **Figure 2** and **Table 1**. The systemic exposure (peak plasma concentration (C_{max}) and area under the curve (AUC)) of MDZ and 1'-hydroxymidazolam was higher when MDZ was coadministered with fenebrutinib compared with MDZ alone. The MDZ C_{max} was ~1.74-fold higher and the area under the plasma concentration-time curve from time point 0 to the end of the dosing interval (AUC_{0-t}) was ~1.99-fold higher following MDZ coadministered with fenebrutinib compared with MDZ alone. Similarly, for 1'-hydroxymidazolam, the C_{max} was ~1.30-fold higher and the AUC_{0-t} was ~1.36-fold higher following MDZ coadministered with fenebrutinib compared with MDZ alone.

Effect of multiple doses of fenebrutinib on the PKs of simvastatin and simvastatin acid

The effect of multiple doses of fenebrutinib 200 mg b.i.d. on the plasma concentration-time profiles of the OATP1B and CYP3A substrate simvastatin and its metabolite simvastatin acid are presented in **Figure 3** and **Table 1**. For simvastatin, the C_{max} was ~1.93-fold higher and the AUC_{0-t} was ~.48-fold higher following simvastatin coadministered with fenebrutinib compared with simvastatin alone. Similarly, for simvastatin acid, the C_{max} was ~1.68-fold higher and the AUC_{0-t} was ~2.71-fold higher following simvastatin coadministered with fenebrutinib compared with simvastatin alone (**Figure 3**).

Effect of multiple doses of fenebrutinib on the PKs of rosuvastatin

The effect of multiple doses of fenebrutinib 200 mg b.i.d. on the plasma concentration-time profiles of the BCRP and OATP1B substrate rosuvastatin are presented in **Figure 4** and **Table 1**. The mean systemic exposure to rosuvastatin was higher following coadministration of rosuvastatin with fenebrutinib compared with following administration of rosuvastatin alone, as assessed from the C_{max} and AUC values. For rosuvastatin, the C_{max} was ~4.99-fold higher and the AUC_{0-t} was ~2.66-fold higher following rosuvastatin coadministered with fenebrutinib compared with rosuvastatin alone.

Effect of fenebrutinib on CP-I and CP-III biomarkers

The effect of multiple doses of fenebrutinib 200 mg b.i.d. on the plasma concentration-time profiles of the BCRP and OATP1B substrate rosuvastatin are presented in **Figure 5**. Following administration of rosuvastatin alone, CP-I levels ranged from 564–680 pg/mL and CP-III levels ranged from 61.0–80.7 pg/mL. Following coadministration of rosuvastatin and fenebrutinib, CP-I levels ranged from 599–768 pg/mL and CP-III levels ranged from 60.9–85.7 pg/mL. CP-I and CP-III levels were comparable following coadministration of rosuvastatin and fenebrutinib compared with following administration of rosuvastatin alone.

DISCUSSION

In this study, *in vitro* experiments to assess the DDI potential of fenebrutinib on metabolic enzymes and transporters were performed, and the results suggested that it may inhibit CYP3A, OATP1B, and BCRP at clinically relevant concentrations. Clinical DDI studies were then conducted to evaluate the presence and magnitude of an interaction using three probe substrates for these elimination pathways. In order to further understand the mechanisms of the observed DDIs, the plasma levels of two endogenous transporter biomarkers were measured in the presence and absence of fenebrutinib.

In vitro results indicated that fenebrutinib has the potential to inhibit CYP3A (k_{inact}/K_i ratio of 1.4 mL/minute/μmol) and transporters *in vivo*. The IC_{50} values for the hepatic uptake transporters OATP1B1 and OATP1B3 were 19.7 μM and 7.15 μM, respectively. Conversely, there was no evidence of inhibition of OAT3 uptake transporter at clinically relevant concentrations. Fenebrutinib also inhibited BCRP efflux transport with an IC_{50}

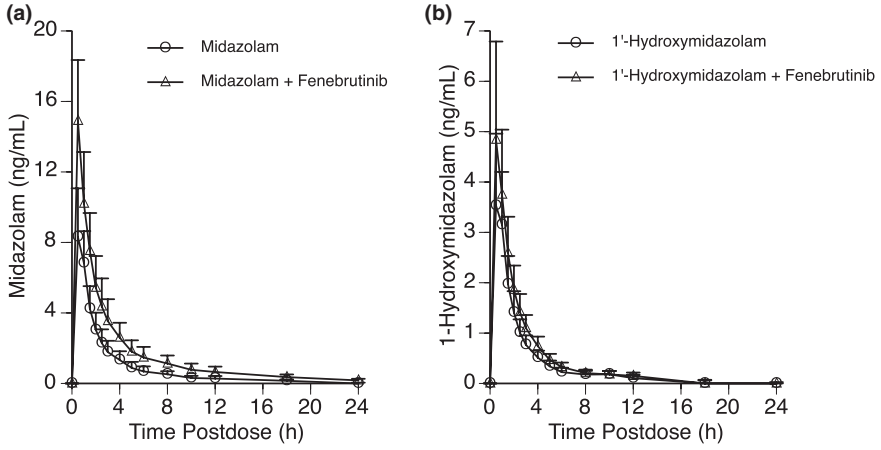

Figure 2 Effect of fenebrutinib on plasma concentrations of midazolam (MDZ) and 1'-hydroxymidazolam. (**a**) Open circle represents single dose of 2 mg MDZ alone (day 1); open triangle represents 2 mg MDZ coadministered with morning b.i.d. 200 mg fenebrutinib (day 9). (**b**) Open circle represents single dose of 2 mg 1'-hydroxymidazolam alone (day 1); open triangle represents 2 mg 1'-hydroxymidazolam coadministered with morning b.i.d. 200 mg fenebrutinib (day 9). Symbols and vertical bars represent arithmetic means and SDs (n = 14–15).

Table 1 PK parameters of MDZ, simvastatin, and rosuvastatin in the presence and absence of 200 mg fenebrutinib in the clinical DDI study

	MDZ			Simvastatin			Rosuvastatin		
Parameter (units)	Control	Fenebrutinib	GMR[a]	Control	Fenebrutinib	GMR[a]	Control	Fenebrutinib	GMR[a]
AUC_{0-t} (hr ng/mL)	19.2 (32.6)	38.3 (30.0)	1.99 (1.80–2.22)	30.2 (40.3)	75.0 (41.1)	2.48 (2.01–3.07)	91.0 (53.3)	226 (55.2)	2.66 (2.37–2.98)
$AUC_{0-\infty}$ (hr ng/mL)	20.5 (31.9)	39.7 (29.7)	1.93 (1.75–2.14)	31.5 (40.1)	78.4 (41.2)	2.49 (2.00–3.09)	93.0 (52.7)	228 (54.5)	2.63 (2.35–2.94)
C_{max} (ng/mL)	8.54 (25.2)	14.8 (23.8)	1.74 (1.58–1.91)	5.20 (51.4)	10.0 (61.4)	1.93 (1.63–2.28)	9.08 (67.8)	43.1 (80.2)	4.99 (3.90–6.40)
$t_{1/2}$[b] (hr)	6.23 (2.23)	6.68 (1.56)	–	8.28 (2.86)	9.32 (4.13)	–	19.9 (7.87)	18.2 (4.92)	–

Geometric mean (geometric percentage of coefficient of variation) are presented unless otherwise indicated.
AUC_{0-t}, area under the curve from time point 0 to the end of the dosing interval; $AUC_{0-\infty}$, area under the curve from 0 to infinity; C_{max}, maximum concentration; DDI, drug–drug interaction; GMR, geometric mean ratio; MDZ, midazolam; PK, pharmacokinetic; $t_{1/2}$, terminal half-life.
[a]GMR (90% confidence interval) are presented. [b]Arithmetic mean (SD) presented for $t_{1/2}$.

of 9.40 μM. *In vitro-in vivo* extrapolation of the observed *in vitro* inhibition potency suggested potential clinical DDIs via CYP3A, OATP1B, and BCRP (**Supplementary Text S1** and **Table S1**). It is important to note that the static prediction methods utilized here are developed for early assessment of clinical DDI potential and not intended for quantitatively predicting the magnitude of DDIs. These results prompted investigation of the potential for interactions in clinical studies.[8]

To evaluate the magnitude of any clinical DDI, a multiple-arm DDI study was performed. MDZ and simvastatin were chosen consistent with their use as commonly evaluated CYP3A probes; additionally, simvastatin was selected for evaluation in this study as it is commonly used in many patient populations and it is also an OATP1B substrate. Rosuvastatin was selected as a multitransporter probe substrate, with its disposition being determined mainly by OATP1B and BCRP, as well as NTCP, OAT3, and CYP2C9.[11] The PKs of single doses of MDZ, simvastatin, or rosuvastatin were assessed prior to and following dosing of fenebrutinib to steady-state. The dosing of fenebrutinib of 200 mg b.i.d. was chosen as this was a dose expected to have the highest likelihood of clinical activity, and it was also the highest clinical dose planned. The observed C_{max} at steady-state with 200 mg b.i.d. in this study was ~1 μM (data not shown).

The magnitude of interaction of fenebrutinib, dosed at 200 mg b.i.d., with MDZ and simvastatin indicated that it is a weak-moderate CYP3A inhibitor based on the definition of a weak, moderate, or strong inhibitor causing increases of > 1.25 to < 2-fold, > 2 to < 5-fold, or > 5-fold in AUC of the probe substrate.[14] For MDZ, the mean C_{max} value was ~1.74-fold higher and the AUC_{0-t} value was ~1.99-fold higher after fenebrutinib administration, suggesting that fenebrutinib can be classified as a weak inhibitor of CYP3A. Coadministration of fenebrutinib with simvastatin resulted in a mean C_{max} value of simvastatin that was 1.93-fold higher and an AUC_{0-t} value that was ~2.48-fold higher compared with simvastatin administered alone. Previous investigations have suggested that simvastatin has lower intestinal availability (F_aF_g) than MDZ (19% vs. 48%)[15]; hence, inhibition of intestinal CYP3A will result in a greater impact to systemic simvastatin exposure compared with systemic MDZ exposure. The observed differences in the effect size of fenebrutinib on MDZ and simvastatin and the minimal change in MDZ $t_{1/2}$ suggest that there is a greater degree of inhibition of intestinal CYP3A compared with hepatic CYP3A. Taken together, the available data suggest that fenebrutinib may be classified as a weak CYP3A inhibitor, except for CYP3A substrates that have relatively low F_g values (e.g., simvastatin) where inhibition may be moderate. Of note, even more pronounced differences in the magnitude of simvastatin interaction and MDZ interaction have been observed with other CYP3A inhibitors.[16] Physiologically-based pharmacokinetic models might be used in such cases to make quantitative prediction of differential DDI outcomes with different CYP3A substrates.

Interestingly, exposures of 1-hydroxymidazolam increased, even though the metabolite/parent ratio decreased as expected. Although the reduction of metabolite/parent ratio is consistent with the reduced CYP3A activity by fenebrutinib, this does not

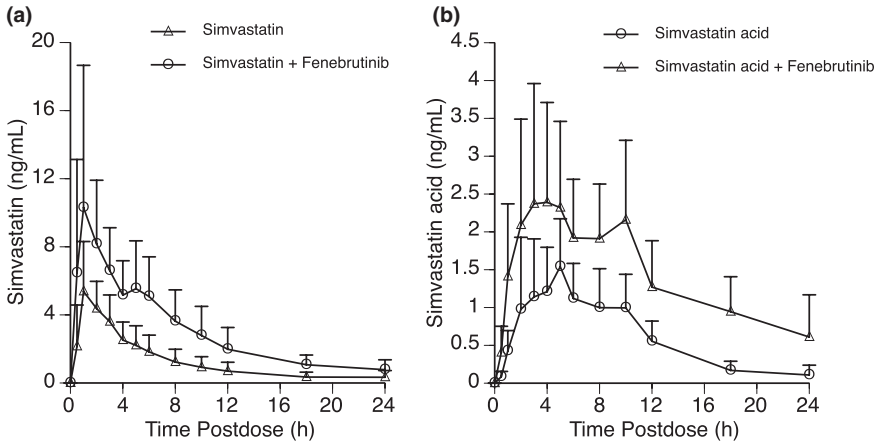

Figure 3 Effect of fenebrutinib on plasma concentrations of simvastatin and simvastatin acid. (**a**) Open circle represents single dose of 40 mg simvastatin alone (day 1); open triangle represents 40 mg simvastatin coadministered with morning b.i.d. 200 mg fenebrutinib (day 9). (**b**) Open circle represents single dose of 40 mg simvastatin acid alone (day 1); open triangle represents 40 mg simvastatin acid coadministered with morning b.i.d. 200 mg fenebrutinib (day 9). Symbols and vertical bars represent arithmetic means and SDs (*n* = 12–16).

explain the increase in the metabolite exposure. Studies using other CYP3A inhibitors reported similar observations, where 1'-hydroxymidazolam exposure was increased to ~1.5-fold in the presence of fluconazole and voriconazole.[17,18] To fully explain the observed interaction, additional mechanisms may need to be considered, such as the inhibition of 1'-hydroxymidazolam elimination via UDP-glucuronosyltransferase.[19]

The observed fenebrutinib–rosuvastatin interaction suggests that fenebrutinib is an *in vivo* transporter inhibitor. Because rosuvastatin is a dual substrate of OATP1B and BCRP, and fenebrutinib inhibits both of these transporters, it was not immediately apparent whether one of the transporters had a greater contribution to the observed DDI. OAT3, the key transporter responsible for renal elimination of rosuvastatin, was not inhibited at a clinically relevant concentration of fenebrutinib. Therefore, we measured the levels of the CP-I and CP-III in the presence and absence of fenebrutinib. As described in the Introduction, they are endogenous substrates of OATP1B transporters. Notably, CP-I is sensitive enough to detect even mild inhibition of OATP1B based on plasma C_{max} and AUC over a 6-hour period postdosing.[20–22] CP-I and CP-III concentrations did not change significantly after fenebrutinib administration to steady-state. This suggests that the main mechanism of the observed DDI was due to the inhibition of intestinal BCRP rather than OATP1B. There are other observations supporting this mechanistic interpretation. First, the observed magnitude of the interaction is consistent with F_aF_g of rosuvastatin. Tanaka *et al.*[23] estimated F_aF_g to be 0.28, which translates to a maximum AUC increase of 3.6-fold if F_aF_g increased to 1 with intestinal BCRP inhibition. Second, increase of C_{max} was more pronounced than AUC_{0-t} (4.99-fold vs. 2.66-fold), and $t_{1/2}$ was comparable, suggesting intestinal availability was altered rather than systemic elimination. Third, intestinal concentration of fenebrutinib is likely higher than hepatic concentration. With similar *in vitro* IC_{50} values between OATP1B and BCRP, it is likely that inhibition of intestinal BCRP is more pronounced than hepatic OATP1B.

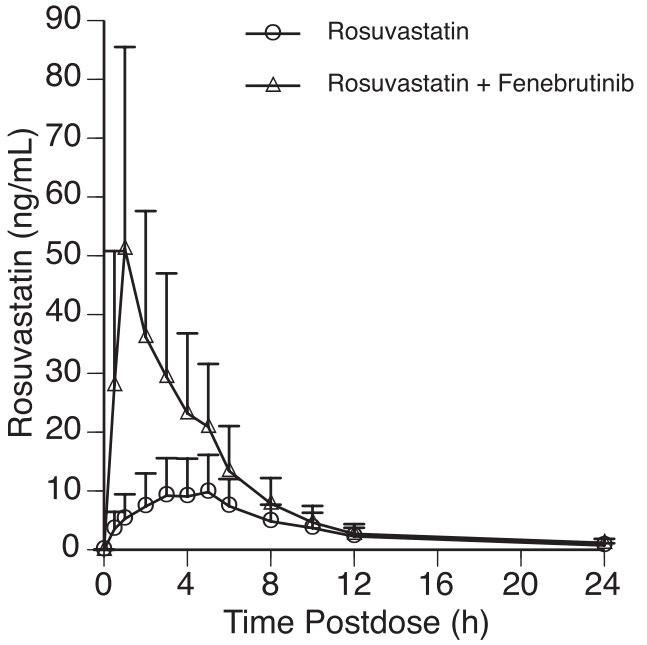

Figure 4 Effect of fenebrutinib on plasma concentrations of rosuvastatin. Open circle represents single dose of 20 mg rosuvastatin alone (day 1); open triangle represents 20 mg rosuvastatin coadministered with morning b.i.d. 200 mg fenebrutinib (day 12). Symbols and vertical bars represent arithmetic means and SDs (*n* = 16).

This mechanistic understanding has important implications on recommendations regarding the use of concomitant medications with fenebrutinib, as there are relatively few BCRP substrates with compelling clinical evidence of DDIs used in autoimmune populations.[24] Conversely, there are many established OATP1B substrates that are widely used in a clinical setting, such as statins, and the restrictions with regard to concomitant administration of fenebrutinib and other medications may have been more extensive had the CP-I and CP-III results indicated that fenebrutinib was an OATP1B inhibitor.[25]

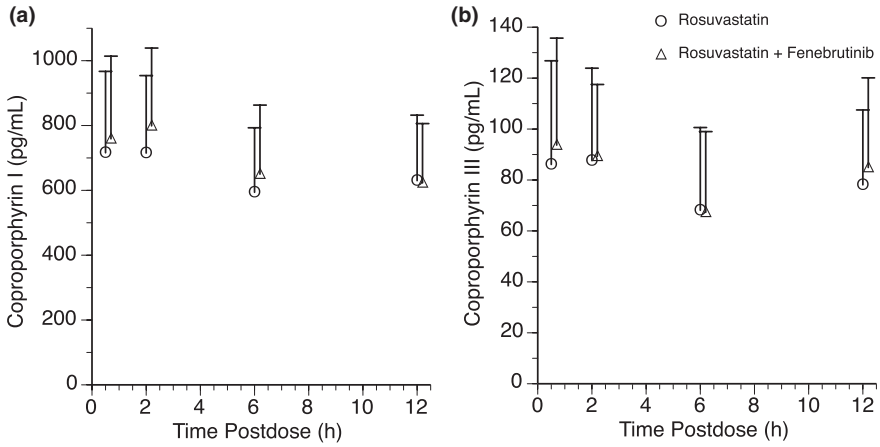

Figure 5 Coproporphyrin (CP)-I and CP-III levels following administration of rosuvastatin with and without fenebrutinib. Open circle represents single dose of 20 mg rosuvastatin alone (day 1); open triangle represents 20 mg rosuvastatin coadministered with morning b.i.d. 200 mg fenebrutinib (day 12). Symbols and vertical bars represent arithmetic means and SDs (n = 15–16).

To our knowledge, this is the first study to elucidate the mechanism of complex clinical DDIs using endogenous transporter biomarkers. Transporter biomarkers have been tools of interest in the field in recent years, but the focus has been mostly to reproduce clinical DDIs observed with probe substrates.[20–22,26] The novel approach taken in this study can broaden the areas of application of endogenous biomarkers. This is especially important for transporter-mediated DDIs, in which many of the chemical probe substrates are also substrates of other transporters, making the mechanistic interpretation of observed DDIs challenging.[6] One example is the DDI between eltrombopag and rosuvastatin. Similar to fenebrutinib, eltrombopag is a potent *in vitro* inhibitor of the OATP1B and BCRP transporters, and a clinical DDI study demonstrated that rosuvastatin exposure was increased by 55% in the presence of eltrombopag.[27] In view of these findings, the product label of Promacta (eltrombopag) states that caution should be taken when concomitantly administering eltrombopag with drugs that are substrates of OATP1B1 (e.g., rosuvastatin and simvastatin acid) or BCRP (e.g., imatinib, methotrexate, and rosuvastatin).[28] In cases such as this one in which the underlying mechanism of a DDI is unclear, the measurement of biomarkers (transporters or enzymes) can provide direct evidence of the clinical DDI mechanisms, as is demonstrated in the present study, and will ideally result in more specific product label recommendations. In such cases, potential disadvantages of endogenous biomarkers should also be noted; CP biomarkers, when used as OATP1B probes in the current study, are also susceptible to perturbation from multidrug resistance protein inhibition.

In summary, this study demonstrated that fenebrutinib is a weak inhibitor of CYP3A using an index substrate, MDZ, at dose levels currently under evaluation in the clinic. Fenebrutinib also increased exposure of rosuvastatin, and further examination, including biomarker measurement, suggested that this DDI is caused by the inhibition of intestinal BCRP, but not of OATP1B or OAT3. This study provided a novel approach of using transporter endogenous biomarkers to understand the mechanism of DDIs where multiple pathways can be involved in the interaction.

METHODS

Reagents

Estrone-3-sulfate, $E_2$17ßG, CCK-8, 1'-hydroxymidazolam, testosterone, and rifampicin were from Sigma-Aldrich (St. Louis, MO). The ^{3}H-Estrone-3-sulfate was from Radiolab (Szeged, Hungary). $E_2$17ßG (estradiol-6,7-^{3}H(N)) and ^{3}H-cholecyctokinine-8 were from Perkin Elmer (Waltham, MA). The 6ß-hydroxytestosterone and pooled human liver microsomes were from BD Biosciences (San Jose, CA). MDZ was from Spectrum Chemicals (New Brunswick, NJ).

In vitro inhibition experiments for uptake transporters

Uptake experiments were performed using HEK293 cells stably expressing human OATP1B1, OATP1B3, or OAT3. Uptake experiments were carried out at 37°C HK buffer (pH 7.4) containing the probe substrate and fenebrutinib or solvent (dimethylsulfoxide). The probe substrates were 1 µM $E_2$17ßG for OATP1B1, 0.1 µM CCK-8 for OATP1B3, and 1 µM estrone-3-sulfate for OAT3. Mock-transfected HEK293 served as control cells. After the experiment, cells were washed twice with 100 µL of HK buffer and lysed with 0.1 M NaOH. The total radioactivity associated with the cell specimens was determined by liquid scintillation counting. Transporter-specific uptake was calculated as the amount of probe substrate in transfected cells in the presence of fenebrutinib minus that in control cells.

In vitro inhibition experiments for BCRP

Transcellular-transport experiments were performed using MDCKII cells stably expressing human BCRP. Cells were pre-incubated in assay buffer for 10 minutes, then assay buffer with prazosin (1 µM, for BCRP) was added to the appropriate apical or basolateral chambers. Bidirectional transport of prazosin in parental and MDCKII-BCRP cell monolayers was determined in the presence and absence of fenebrutinib on both chambers. After incubation (60 minutes at 37°C), aliquots were taken from the receiver chambers to determine the amount of translocated prazosin. Samples containing prazosin were analyzed by scintillation counting. The IC_{50} value were calculated using the relative efflux ratio, defined as (the efflux ratio in the presence of the inhibitor − 1)/(the efflux ratio in the absence of the inhibitor − 1).

In vitro inhibition experiments for CYP enzymes

To determine reversible CYP inhibition, fenebrutinib was pre-incubated at 37°C for 10 minutes with human liver microsomes containing

Table 2 Demographics of the study participants

Demographic	Part 1 (*N* = 16)	Part 2 (*N* = 16)	Part 3 (*N* = 15)
Mean age, years (min, max)	46 (26, 58)	49 (28, 61)	42 (20, 60)
Mean weight, kg (min, max)	76.84 (63.25, 92.05)	75.56 (50.10, 99.95)	82.65 (69.30, 98.50)
Mean height, cm (min, max)	167.2 (153.8, 182.6)	170.7 (154.8, 184.1)	178.0 (165.0, 195.1)
Mean BMI, kg (min, max)	27.52 (22.01, 30.72)	25.72 (20.67, 30.61)	26.11 (21.15, 28.78)
Sex, *n* (%)			
Male	9 (56.3)	10 (62.5)	13 (86.7)
Female	7 (43.8)	6 (37.5)	2 (13.3)
Race, *n* (%)			
Asian		2 (12.5)	
Black or African American	5 (31.3)	3 (18.8)	5 (33.3)
American white	11 (68.8)	11 (68.8)	10 (66.7)
Ethnicity, *n* (%)			
Hispanic or Latino	10 (62.5)	3 (18.8)	2 (13.3)
Not Hispanic or Latino	6 (37.5)	13 (81.3)	13 (86.7)

BMI, body mass index; max, maximum; min, minimum; *N*, number of subjects; *n*, number of observations; %, *n/N**100.

a substrate selective for a specific CYP isoform. The incubations were initiated by the addition of reduced B nicotinamide adenine dinucleotide phosphate (NADPH; 1.3 mM). Following incubation, the reactions were quenched with 3% formic acid in acetonitrile containing internal standard and analyzed by liquid chromatography tandem mass spectrometry (LC-MS/MS) for CYP-specific metabolite formation. The amount of metabolites formed at each concentration relative to control (or the percent remaining activity) was calculated as follows:

$$\%\text{control activity} = \text{peak area ratio with compound} / \text{peak ratio without compound} \times 100$$

The kinetic parameters of fenebrutinib time-dependent inhibition of CYP3A were determined using both MDZ and TST as probe substrates. Fenebrutinib was pre-incubated with human liver microsomes (0.6 mg/mL) in the presence of NADPH (1.3 mM) for 0.5, 2.5, 9, 16, and 25 minutes at 37°C. After pre-incubation, a 20-fold dilution was performed in a secondary incubation containing NADPH (1.3 mM) and MDZ or TST at a final concentration of 50 or 250 µM, respectively. The secondary assay was allowed to proceed for 4 minutes at 37°C for each probe substrate. Reactions were quenched with 3% formic acid in acetonitrile containing internal standard and analyzed by LC-MS/MS for CYP-specific metabolite formation. The time-dependent and concentration-dependent inhibition was characterized by the k_{inact} and apparent K_I, calculated by fitting the observed inactivation rate constant against inhibitor concentrations with the following equation:

$$k_{obs} = \frac{[I] \times k_{kinact}}{[I] + K_I}$$

Clinical DDI study to evaluate fenebrutinib as enzyme and transporter inhibitor

This study was a phase I, open-label, nonrandomized, multisite, DDI study in healthy male and female (of nonchildbearing potential) subjects to evaluate the effect of fenebrutinib on the PKs of MDZ and its metabolite 1'-hydroxymidazolam (part 1), rosuvastatin (part 2), and simvastatin and its metabolite simvastatin acid (part 3). The demographics of study participants are presented in **Table 2**. This study was conducted according to US Food and Drug Administration regulations, the International Conference on Harmonisation E6 Guideline for Good Clinical Practice (which are consistent with the Declaration of Helsinki), and applicable local, state, and federal laws.

Each part of the study was a three-period fixed-sequence design in which period 1 consisted of a single dose of the victim drug (2 mg MDZ, 20 mg rosuvastatin, or 40 mg simvastatin), period 2 consisted of multiple doses of the fenebrutinib to steady-state (6 days of b.i.d. oral doses of 200 mg), and period 3 consisted of a single dose of the victim drug in combination with multiple doses fenebrutinib. For each part, potential subjects were screened to assess their eligibility to enter the study within 27 days (days −28 to −2) prior to study entry. Eligible subjects were admitted to the Clinical Research Unit on day −1 (check-in) and confined for up to 16 days (depending on the study part), followed by a telephone call 28 days after the last dose administered. Blood samples for PK analysis of victim drugs and fenebrutinib were collected predose and at specified times after victim drug administrations. Additional blood samples for PK analysis of trough concentrations of fenebrutinib were collected to verify that steady-state had been achieved prior to coadministration and that steady-state was maintained thereafter. Detailed description on the schedule of drug administration and sample collection can be found in the **Supplementary Text S2**.

Plasma concentrations of analytes evaluated in this study were determined using validated bioanalytical methods at Covance Laboratories (Madison, WI). Concentrations of analytes in human plasma containing K2EDTA as an anticoagulant were determined using supported-liquid extraction (fenebrutinib, rosuvastatin, simvastatin, and simvastatin acid) and liquid-liquid extraction (MDZ, 1'-hydroxymidazolam, CP-I, and CP-III) followed by analysis using high-performance LC-MS/MS detection. The lower limit of quantification was 0.5 ng/mL for fenebrutinib, 0.1 ng/mL for MDZ, 0.1 ng/mL for 1'-hydroxymidazolam, 0.02 ng/mL for rosuvastatin, 0.05 ng/mL for simvastatin, 0.05 ng/mL for simvastatin acid, 50 pg/mL for CP-I, and 20 pg/mL for CP-III. Analysis runs for all analytes were determined to have a high degree of reproducibility and acceptably low inter-run carryover, which was considered acceptable for PK quantification.

To evaluate the effect of coadministration of fenebrutinib on the PK of MDZ, 1'-hydroxymidazolam, rosuvastatin, simvastatin, and simvastatin acid, the PK parameters C_{max}, AUC_{0-t}, and AUC extrapolated to infinity ($AUC_{0-\infty}$) of the victim drugs (coadministration of victim and fenebrutinib as perpetrator; test treatment) were compared with the administration of victim alone (reference treatment). The PK parameters

were log transformed (base e) prior to analysis and were analyzed using a mixed model. The model included treatment as a fixed effect and subject as a random effect. For $AUC_{0-\infty}$, AUC_{0-t}, and C_{max}, least square means were calculated for the test and reference treatments. Mean differences between the test and reference treatments were calculated. The residual variance from the mixed model was used to calculate 90% confidence interval for the difference between the test and reference treatments. These values were back-transformed to give geometric least square means, a point estimate, and 90% confidence interval for the ratio of the test treatment relative to the reference treatment.

SUPPORTING INFORMATION

Supplementary information accompanies this paper on the *Clinical Pharmacology & Therapeutics* website (www.cpt-journal.com).

Supplementary Material: Supplementary Texts and Table S1.

ACKNOWLEDGMENTS

The authors acknowledge Srilatha Swami, Mausumi Debnath, Harbeen Grewal, and Peter Malloy for medical writing support of this manuscript.

FUNDING

The work described in this manuscript was funded by Genentech, Inc.

CONFLICT OF INTEREST

All authors are employees and stockholders of Genentech, Inc.

AUTHOR CONTRIBUTIONS

N.J., K.Y., L.S., J.K., M.D., and L.C. wrote the manuscript. K.Y., L.S., J.K., M.D., and L.C. designed the research. N.J., K.Y., L.S., J.K., and M.D. performed the research. N.J., K.Y., L.S., J.K., M.D., and L.C. analyzed the data.

1. International Transporter, C. *et al*. Membrane transporters in drug development. *Nat. Rev. Drug Discov.* **9**, 215–236 (2010).
2. US Food and Drug Administration. Draft guidance/In Vitro Metabolism- and Transporter- Mediated Drug-Drug Interaction Studies Guidance for Industry <https://www.fda.gov/downloads/Drugs/Guidances/UCM581965.pdf> (2017). Accessed April 19, 2019.
3. European Medicines Agency. Guideline on the investigation of drug interactions <https://www.ema.europa.eu/en/documents/scientific-guideline/guideline-investigation-drug-interactions_en.pdf> (2012). Accessed April 19, 2019.
4. Ministry of Health Labour and Welfare Japan. Guideline of drug interaction studies for drug development and appropriate provision of information <https://www.pmda.go.jp/files/000228122.pdf%3E>. Accessed April 19, 2019.
5. Vaidyanathan, J., Yoshida, K., Arya, V. & Zhang, L. Comparing various in vitro prediction criteria to assess the potential of a new molecular entity to inhibit organic anion transporting polypeptide 1B1. *J. Clin. Pharmacol.* **56**(suppl. 7), S59–S72 (2016).
6. Chu, X. *et al*. Clinical probes and endogenous biomarkers as substrates for transporter drug–drug interaction evaluation: perspectives from the international transporter consortium. *Clin. Pharmacol. Ther.* **104**, 836–864 (2018).
7. Bednarczyk, D. & Boiselle, C. Organic anion transporting polypeptide (OATP)-mediated transport of coproporphyrins I and III. *Xenobiotica* **46**, 457–466 (2016).
8. Crawford, J.J. *et al*. Discovery of GDC-0853: a potent, selective, and noncovalent Bruton's tyrosine kinase inhibitor in early clinical development. *J. Med. Chem.* **61**, 2227–2245 (2018).
9. Herman, A.E. *et al*. Safety, pharmacokinetics, and pharmacodynamics in healthy volunteers treated with GDC-0853, a selective reversible Bruton's tyrosine kinase inhibitor. *Clin. Pharmacol. Ther.* **103**, 1020–1028 (2018).
10. Pfeifer, N.D., Yang, K. & Brouwer, K.L. Hepatic basolateral efflux contributes significantly to rosuvastatin disposition I: characterization of basolateral versus biliary clearance using a novel protocol in sandwich-cultured hepatocytes. *J. Pharmacol. Exp. Ther.* **347**, 727–736 (2013).
11. Wang, Q., Zheng, M. & Leil, T. Investigating transporter-mediated drug–drug interactions using a physiologically based pharmacokinetic model of rosuvastatin. *CPT Pharmacometrics Syst. Pharmacol.* **6**, 228–238 (2017).
12. Zamek-Gliszczynski, M.J. *et al*. Transporters in drug development: 2018 ITC recommendations for transporters of emerging clinical importance. *Clin. Pharmacol. Ther.* **104**, 890–899 (2018).
13. Elsby, R., Hilgendorf, C. & Fenner, K. Understanding the critical disposition pathways of statins to assess drug-drug interaction risk during drug development: it's not just about OATP1B1. *Clin. Pharmacol. Ther.* **92**, 584–598 (2012).
14. US Food and Drug Administration. Draft guidance/Clinical Drug Interaction Studies—Study Design, Data Analysis, and Clinical Implications Guidance for Industry <https://www.fda.gov/downloads/drugs/guidances/ucm292362.pdf> (2017). Accessed April 19, 2019.
15. Hisaka, A., Nakamura, M., Tsukihashi, A., Koh, S. & Suzuki, H. Assessment of intestinal availability (FG) of substrate drugs of cytochrome p450s by analyzing changes in pharmacokinetic properties caused by drug-drug interactions. *Drug Metab. Dispos.* **42**, 1640–1645 (2014).
16. Hoch, M., Hoever, P., Alessi, F., Theodor, R. & Dingemanse, J. Pharmacokinetic interactions of almorexant with midazolam and simvastatin, two CYP3A4 model substrates, in healthy male subjects. *Eur. J. Clin. Pharmacol.* **69**, 523–532 (2013).
17. Ahonen, J., Olkkola, K.T. & Neuvonen, P.J. Effect of route of administration of fluconazole on the interaction between fluconazole and midazolam. *Eur. J. Clin. Pharmacol.* **51**, 415–419 (1997).
18. Saari, T.I., Laine, K., Leino, K., Valtonen, M., Neuvonen, P.J. & Olkkola, K.T. Effect of voriconazole on the pharmacokinetics and pharmacodynamics of intravenous and oral midazolam. *Clin. Pharmacol. Ther.* **79**, 362–370 (2006).
19. Nguyen, H.Q., Kimoto, E., Callegari, E. & Obach, R.S. Mechanistic modeling to predict midazolam metabolite exposure from in vitro data. *Drug Metab. Dispos.* **44**, 781–791 (2016).
20. King-Ahmad, A. *et al*. A fully automated and validated human plasma LC-MS/MS assay for endogenous OATP biomarkers coproporphyrin-I and coproporphyrin-III. *Bioanalysis* **10**, 691–701 (2018).
21. Kunze, A., Ediage, E.N., Dillen, L., Monshouwer, M. & Snoeys, J. Clinical investigation of coproporphyrins as sensitive biomarkers to predict mild to strong OATP1B-mediated drug–drug interactions. *Clin. Pharmacokinet.* **57**, 1559–1570 (2018).
22. Liu, L. *et al*. Effect of OATP1B1/1B3 inhibitor GDC-0810 on the pharmacokinetics of pravastatin and coproporphyrin I/III in healthy female subjects. *J. Clin. Pharmacol.* **58**, 1427–1435 (2018).
23. Tanaka, Y., Kitamura, Y., Maeda, K. & Sugiyama, Y. Quantitative analysis of the ABCG2 c.421C>A polymorphism effect on in vivo transport activity of breast cancer resistance protein (BCRP) using an intestinal absorption model. *J. Pharm. Sci.* **104**, 3039–3048 (2015).
24. Lee, C.A. *et al*. Breast cancer resistance protein (ABCG2) in clinical pharmacokinetics and drug interactions: practical recommendations for clinical victim and perpetrator drug-drug interaction study design. *Drug Metab. Dispos.* **43**, 490–509 (2015).
25. US Food and Drug Administration. Drug Development and Drug Interactions: Table of Substrates, Inhibitors and Inducers

<https://www.fda.gov/Drugs/DevelopmentApprovalProcess/DevelopmentResources/DrugInteractionsLabeling/ucm093664.htm> (2017). Accessed May 7, 2019.

26. Lai, Y. *et al*. Coproporphyrins in plasma and urine can be appropriate clinical biomarkers to recapitulate drug–drug interactions mediated by organic anion transporting polypeptide inhibition. *J. Pharmacol. Exp. Ther.* **358**, 397–404 (2016).
27. Allred, A.J. *et al*. Eltrombopag increases plasma rosuvastatin exposure in healthy volunteers. *Br. J. Clin. Pharmacol.* **72**, 321–329 (2011).
28. US Food and Drug Administration. Promacta: Highlights of prescribing information <https://www.accessdata.fda.gov/drugsatfda_docs/label/2017/207027s003lbl.pdf> (2008). Accessed May 7, 2019.